

A Learning-based Model Predictive Control Scheme with Application to Temperature Control Units

Jing Xie^{1,*}, Léo Simpson^{2,*}, Jonas Asprion², Riccardo Scattolini¹

Abstract—Temperature control is a complex task due to its often unknown dynamics and disturbances. This paper explores the use of Neural Nonlinear AutoRegressive eXogenous (NNARX) models for nonlinear system identification and model predictive control of a temperature control unit. First, the NNARX model is identified from input-output data collected from the real plant, and a state-space representation with known measurable states consisting of past input and output variables is formulated. Second, a tailored model predictive controller is designed based on the trained NNARX network. The proposed control architecture is experimentally tested on the temperature control units manufactured by Tool-Temp AG. The results achieved are compared with those obtained using a PI controller and a linear MPC. The findings illustrate that the proposed scheme achieves satisfactory tracking performance while incurring the lowest energy cost among the compared controllers.

Index Terms—Nonlinear Model Predictive Control, Neural Networks, Temperature Control

I. INTRODUCTION

Temperature control is a critical aspect in a wide array of industrial, commercial, and residential applications, ranging from manufacturing processes [1], [2] to climate control systems [3]. The ability to track specific temperature profiles is paramount for ensuring product quality or process efficiency. Temperature control units, also known as temperature controllers, play a pivotal role in achieving precise and stable temperature conditions within diverse operational environments. To that end, temperature control units (TCUs), such as the ones produced by Tool-Temp AG, are used. These devices (see Figure 1) temper the external process by supplying a thermal fluid at a suitable temperature and volumetric flow. Due to their universal applicability, TCUs are often used for different tasks on an hourly to daily basis.

In practical applications, these devices are commonly governed by a PID controller, owing to its ease of implementation and remarkable performance [4]. Nevertheless, PID control exhibits limitations, such as the requirement for precise tuning, sensitivity to system changes, and challenges in handling nonlinear processes [5]. While widely used for their simplicity, these limitations have led to the development and application of more advanced control strategies, e.g., model-based control. The adoption of model-based control strategies provides enhanced flexibility, precision, and adaptability in handling complex systems [6]. Indeed, accurate



Fig. 1. Temperature Control Unit manufactured by Tool-Temp AG

mathematical models are key to the implementation of such control algorithms. The common modeling practice for TCUs heavily relies on physical knowledge, e.g., heat transfer behaviors for thermal systems. Nevertheless, certain variables remain unknown to the TCU controller in the field. These uncertainties include delays attributable to the tubes linking the TCU and external systems, the heat-transfer fluid used and its properties, as well as fluctuations in cooling water temperature and flow rate. All these factors contribute to the complexity of physical modeling, rendering it sensitive to unmodeled uncertainties.

While parametric linear systems could fit those requirements, enlarging the space of possible models with nonlinear ones might increase the modeling performance. To this end, Recurrent Neural Networks (RNNs) emerge as a promising framework, owing to their robust ability to characterize nonlinear behaviors and make accurate time-series predictions. Many RNN model architectures are proposed in the literature, e.g., Long short-term memory networks (LSTM) [7], Gated Recurrent Units (GRU) [8], Echo State Networks (ESN) [9] and Neural NARXs (NNARX) [10].

Regarding model-based control algorithms, Model Predictive Control (MPC) is one of the most popular methods. It uses process models to predict future system behaviors and minimize its cost. At each time step, it solves a finite-dimensional constrained optimization problem, which approximates the optimality condition of the decision [11].

Given the latter discussions on model identification and model-based control, the goal of this paper is twofold. First, it focuses on the system identification of TCUs, including the identification of a linear model, and the training of Neural NARX networks. The choice of NNARX is due to

* Equal contribution

¹ The authors are with Dipartimento di Elettronica, Informazione e Bioingegneria, Politecnico di Milano, Via Ponzio 34/5, 20133, Milano, Italy.

² The authors are with Tool-Temp AG, Industriestrasse 30, 8583, Sulgen, Switzerland.

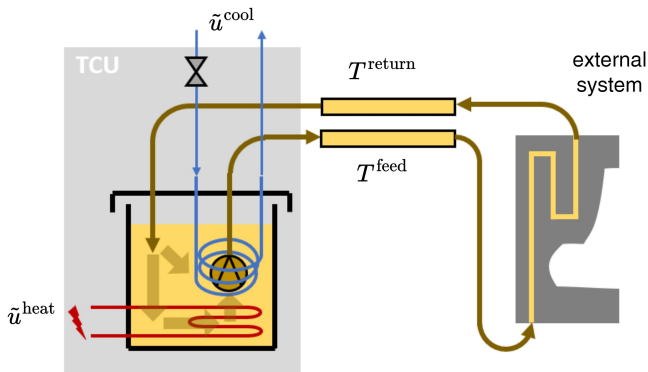


Fig. 2. Overall system with TCU and external system

its simple structure and ease of training. Second, a tailored MPC algorithm, leveraging the learned model, is designed for real-time temperature control of TCUs with tracking and economic objectives. The paper is organized as follows. In Section II, the physical system of TCU is described, and the control problem is formulated. In Section III the training procedure is introduced. In Section IV, a tailored nonlinear MPC algorithm is designed for real-time implementation. In Section V, the experiments are conducted on TCUs, and performances of nonlinear MPC, linear MPC, and PI control are discussed. Lastly, some conclusions are drawn in Section VI.

II. PROBLEM STATEMENT

The objective is to control the output fluid temperature T^{feed} of the TCU to match a predetermined reference temperature r . The TCU operates based on two binary control inputs. The first, named \tilde{u}^{heat} , represents heating by applying a voltage to electrical resistance, whereas the second, namely \tilde{u}^{cool} indicates the binary position of a valve that can let the cooling-water flow through a cooling coil. The fluid, whether water or oil, is fed into an unknown external system at temperature T^{feed} . After going through the unknown thermal process, it returns to the TCU at temperature T^{return} . These two latter temperatures are measured with sensors. This is illustrated in Figure 2.

Every $\Delta t = 1\text{s}$, the binary control input $\tilde{u} = [\tilde{u}^{\text{heat}}, \tilde{u}^{\text{cool}}]$ is executed and T^{feed} is measured by sensors. We denote $u = [u^{\text{heat}}, u^{\text{cool}}] \in [0, 1]^2$ as the analog control input, which is computed by a discrete-time controller. At time step k , an analog input is transformed into a digital one using the delta modulation (DM) [12] defined as follows:

$$\tilde{u}_k^m := \begin{cases} 1 & \text{if } \sum_{i=0}^{k-1} \tilde{u}_i^m < \sum_{i=0}^k u_i^m \\ 0 & \text{else} \end{cases} \quad (1)$$

where $m \in \{\text{heat}, \text{cool}\}$. An example signal of analog-to-digital conversion is depicted in Figure 3.

The system that we choose to identify contains the TCU, the external process, and the analog-to-digital converter.

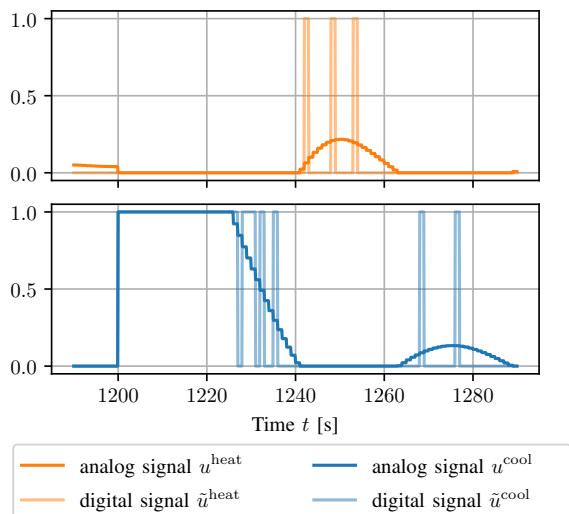


Fig. 3. Analog input signal u together with its digital conversion \tilde{u} .

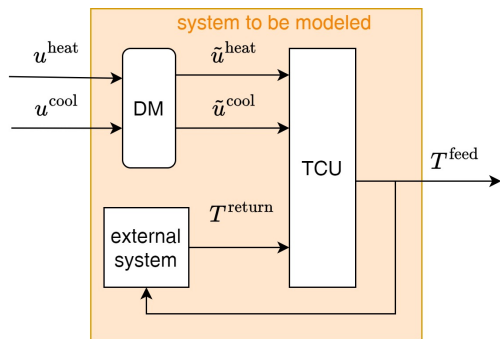


Fig. 4. System abstraction

Hence, it inputs the analog variables u^{heat} and u^{cool} and its single output is T^{feed} . This is depicted in Figure 4.

In the experiments conducted for this paper, the external system is only a closed circuit, that acts as a delay for the temperature of the fluid. As a result, the system is mainly defined by the TCU. However, in other applications of this device, the external system can be any other thermal process.

III. SYSTEM IDENTIFICATION

In this section, we present the system identification procedure that has been conducted. We first describe the experiment design that is used to collect data. In the following parts, we use this data to identify two models: a linear model, and a black-box nonlinear model, using the NNARX structure. The identified models will be used to design a Model Predictive Controller in Section IV.

A. Data Collection using a PI controller

The first step of the model identification procedure is the data collection. For this purpose, we conduct experiments on the real plant, while it is controlled by a simple control algorithm. As opposed to generating inputs randomly, using closed-loop data is advantageous because it can guarantee safety during operation, and it allows to collect data for a

chosen temperature range. Furthermore, the collected data will offer information that is relevant to our control task, such as steady-state information. Note that in the case of closed-loop data, the data is informative as long as the reference signal that the controller tracks is itself persistently exciting [13, Theorem 13.2]. For convenience, the same controller will be used to assess the performance of our control algorithm in the last section of this paper. For this simple controller, we choose a discrete Proportional-Integral (PI) Controller, defined by the following equation

$$u_k^{\text{pi}} = K_p e_k + K_i \sum_{i=0}^k e_i \quad (2)$$

where $e_k := r_k - y_k$ is the tracking error at time step k and $y_k := T_k^{\text{feed}}$ denotes the plant output at time step k . K_i and K_p denote parameters for the PI controller, which are empirically tuned to stabilize the plant. Eventually, u^{pi} is projected in the interval $[-1, 1]$ such that positive (negative) values indicate heating (cooling). This is summarized by the following equations

$$u^{\text{heat}} = \begin{cases} 1, & \text{if } u^{\text{pi}} \geq 1 \\ 0, & \text{if } u^{\text{pi}} \leq 0 \\ u^{\text{pi}}, & \text{else} \end{cases}, \quad u^{\text{cool}} = \begin{cases} 1, & \text{if } u^{\text{pi}} \leq -1 \\ 0, & \text{if } u^{\text{pi}} \geq 0 \\ -u^{\text{pi}}, & \text{else} \end{cases} \quad (3)$$

An anti-windup strategy is also used, where the sum in (2) is not updated when the actuators are saturated. The output reference of PI is piecewise constant, and carefully chosen to generate an informative dataset. The input-output data has been recorded with sampling time $\Delta t = 1\text{s}$ for a total of 11760 time steps. One of the collected sequences is shown in Figure 5. Finally, the data is resampled to $\tau_t = 6\text{s}$ for model identification.

B. Identification of a linear model

Using the collected data, we estimate the parameters of a discrete-time state-space model that takes the following form

$$\begin{aligned} x_{k+1}^1 &= x_k^1 + b_h u_k^{\text{heat}} + b_c u_k^{\text{cool}} + n_1, \\ x_{k+1}^2 &= x_k^2 + a[x_k^1 - x_k^2] + n_2, \\ T_k^{\text{feed}} &= x_k^2 + n_y, \end{aligned} \quad (4)$$

where n_1, n_2, n_y are process and measurement noise, a, b_h, b_c are parameters of the model, and x^1, x^2 are the states of the system. The model parameters together with the noise covariances are estimated from the data using the Maximum Likelihood Estimation (MLE) framework introduced in [14]. The algorithm that is used for the estimation procedure is described in [15]. The identified nominal model can also be written compactly:

$$\Sigma_l : \begin{cases} x_{k+1} = f_l(x_k, u_k) \\ y_k = g_l(x_k) \end{cases} \quad (5)$$

where $u = [u^{\text{heat}}, u^{\text{cool}}]'$ are the input of the system, and $y = T^{\text{feed}}$ is the output.

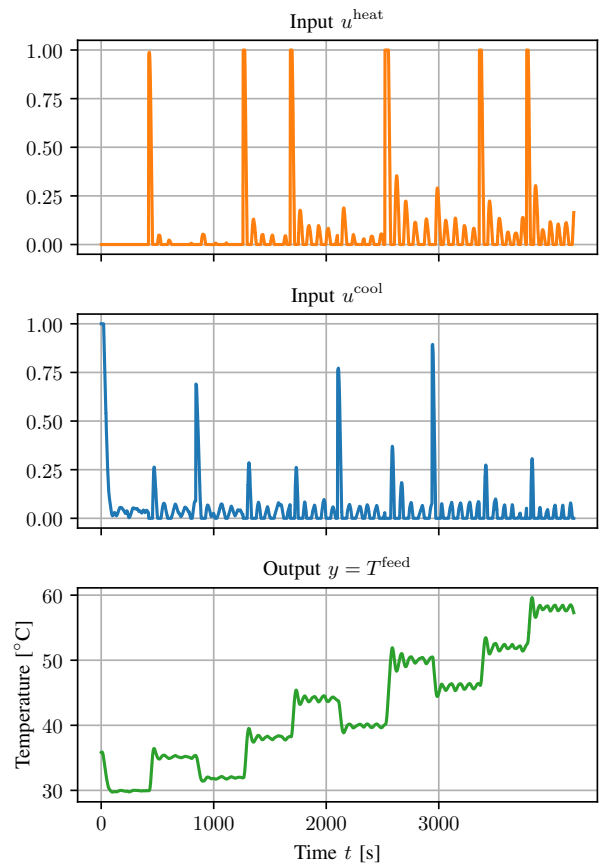


Fig. 5. Exemplary sample of the collected data

C. Neural NARX models

NNARX models [16] are nonlinear, time-invariant, discrete-time models. At time instant k , the future output y_{k+1} is computed as a nonlinear regression function η on past N input $u_k \in \mathbb{R}^m$ and output data $y_k \in \mathbb{R}^p$, i.e.,

$$y_{k+1} = \eta(y_k, y_{k-1}, \dots, y_{k-N+1}, u_k, u_{k-1}, \dots, u_{k-N}; \Phi), \quad (6)$$

where Φ is the training parameters. By defining, for $i \in \{1, \dots, N\}$,

$$z_{i,k} = \begin{bmatrix} y_{k-N+i} \\ u_{k-N+1+i} \end{bmatrix}, \quad (7)$$

and by denoting the state vector $x_k = [z'_{1,k}, \dots, z'_{N,k}]' \in \mathbb{R}^n$, it is straightforward to rewrite model (6) in state space form:

$$\begin{cases} x_{k+1} = Ax_k + B_u u_k + B_x \eta(x_k, u_k; \Phi) \\ y_k = Cx_k \end{cases} \quad (8)$$

where A, B_u, B_x , and C are fixed matrices with known structure and elements equal to zero or one, see [17]. In NNARX models, the regression function η in (6) is described by a Feed-Forward Neural Network (FFNN), which is depicted in Figure 6. Each layer consists of a linear combination of its input and a bias, squashed by a suitable nonlinear function σ , known as the activation function. A compact formulation of η is as follows

$$\eta(x_k, u_k) = U_0 \eta_M(\eta_{M-1}(\dots \eta_1(x_k, u_k), u_k), u_k) + b_0 \quad (9)$$

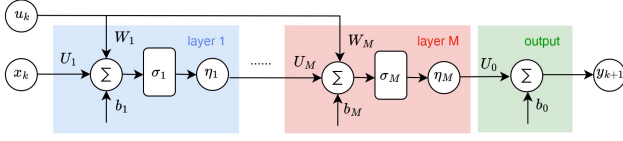


Fig. 6. Structure of the NNARX model

where η_l is the nonlinear relation between l -th and the previous layer, which can be written as

$$\eta_l(\eta_{l-1}, u_k) = \psi_l(W_l u_k + U_l \eta_{l-1} + b_l), \quad (10)$$

ψ_l is an activation function, which is applied element-wise on its argument. We assume that ψ_l is Lipschitz-continuous and satisfying $\psi_l(0) = 0$. The matrices W_l , U_l , and b_l are the learnable weights of the layer, which constitute the network's training parameters

$$\Phi = \{U_0, b_0, \{U_l, W_l, b_l\}_{l=1, \dots, M}\} \quad (11)$$

Henceforth, the NNARX model is denoted as,

$$\Sigma_n : \begin{cases} x_{k+1} = f_n(x_k, u_k) \\ y_k = g_n(x_k) \end{cases}, \quad (12)$$

where the dependency on Φ is omitted for compactness.

D. NNARX model training

The weights Φ as discussed are learned from the input-output data collected in Section III-A, where the weights that best explain the measured data are sought. The activation function is tanh function in this paper, for more details, see [16] for example.

According to the Truncated Back-Propagation Through Time (TBPTT) principle [18], $N_t = 84$ random subsequences of length $N_s = 133$ time steps, denoted by $(\mathbf{u}_{N_s}^{\{i\}}, \mathbf{y}_{p, N_s}^{\{i\}})$, with $i = 1, \dots, N_t$, have been extracted from the experimental data. One other experiment has been performed, from which $N_v = 32$ subsequences have been extracted as independent validation test datasets.

The training procedure has been conducted using PyTorch 1.9. The employed NNARX model is characterized by a single-layer ($M = 1$) FFNN regression function with 10 neurons, and the past $N = 8$ input-output data has been stored in the state. Following the guidelines of [19], [16], the model has been trained by minimizing the Mean Square Error (MSE) of one-step prediction over the training set, defined as follows

$$\mathcal{L}_{\text{MSE}}(\Phi) = \alpha \sum_{i=1}^{N_t} \sum_{k=N_w}^{N_s} \left(y_{k+1}(x_k^{\{i\}}, u_k^{\{i\}}) - y_k^{\{i\}} \right)^2 \quad (13)$$

where $y_{k+1}(x_k^{\{i\}}, u_k^{\{i\}})$ is the one-step prediction defined in (6), $y_k^{\{i\}}$ the measurement value and $\alpha := \frac{1}{N_t(N_s - N_w)}$ is for scaling purposes. N_w denotes the washout length to discount initialization. The NNARX model has been trained until the criterion function (13) evaluated on the validation set

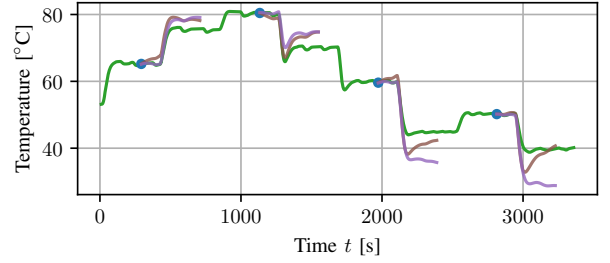


Fig. 7. Open-loop prediction performance

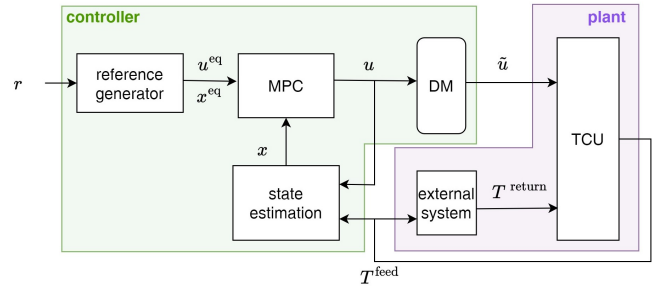


Fig. 8. Schematic of the proposed control architecture

becomes lower than a tolerance, set to 10^{-4} . In the present case, this corresponds to about 1500 epochs.

The open-loop predictions are depicted in Figure 7 to compare the modeling performance of the linear model and NNARX model. The predictions start at four different points with prediction horizon $N_T = 70$ steps. The NNARX model provides better predictions than the linear one due to the past information stored in the state.

IV. CONTROL SCHEME

Now we design a Model Predictive Control (MPC) scheme to control our plant, based on the models identified in the previous section. The schematic diagram of the control scheme is shown in Figure 8.

A. Cost design

The design of the MPC scheme should be driven by the minimization of a stage cost. Our modeling choice for this is the sum of the squared tracking error with a linear input penalization, which represents an economic cost:

$$l(y, u, r) := (y - r)^2 + \lambda \cdot (u^{\text{heat}} + u^{\text{cool}}) \quad (14)$$

where r is the reference signal, u is the input of the system, y is the output of the system and λ is a parameter that we set to $\lambda = 50$. This cost is chosen because the controller needs to not only track the temperature reference signal but also minimize energy consumption while performing this task.

B. Reference generation for input and state

For a certain output temperature reference r , we compute the equilibrium state that minimizes the stage cost (14). This is done by solving the following optimization problem

$$\min_{u,x,y} l(y,u,r) \quad (15a)$$

$$\text{s.t. } x = f(x,u) \quad (15b)$$

$$y = g(x) \quad (15c)$$

The equilibrium state x^{eq} is used in the terminal constraint of the MPC optimization problem, which is defined in Section IV-D.

C. State estimation

In the case of the NNARX model, the state is directly given by past input and past measurements. In the case of the linear system, the state estimation is done via a Kalman Filter that takes into account the noise model that has been estimated (see [15] for more details).

D. Model Predictive Control

An MPC control law is now designed. It relies on solving the following constrained optimization problem for each time step k

$$\begin{aligned} & \underset{\substack{\bar{u}_0, \dots, \bar{u}_{N_p-1}, \\ \bar{x}_0, \dots, \bar{x}_{N_p}}}{\text{minimize}} & \sum_{i=0}^{N_p-1} l(g(\bar{x}_i), \bar{u}_i, r) \end{aligned} \quad (16a)$$

$$\text{subject to} \quad (16b)$$

$$\bar{x}_0 = x \quad (16c)$$

$$\bar{x}_{i+1} = f(\bar{x}_i, \bar{u}_i) \quad \text{for } i = 1, \dots, N_p - 1 \quad (16d)$$

$$\bar{u}_i \in \mathcal{U} \quad \text{for } i = 1, \dots, N_p - 1 \quad (16e)$$

$$\bar{x}_{N_p} = x^{\text{eq}} \quad (16f)$$

In the objective function (16a), $N_p = 30$ denotes the prediction horizon. The feasible input set $\mathcal{U} := [0, 1]^2$ is chosen so that both \bar{u}^{heat} and \bar{u}^{cool} are constrained to be between 0 and 1. The identified model is applied as a predictive model (see (16d)) and it is initialized with the current state value x (see (16c)). Finally, (16f) is introduced as terminal equality constraints to guarantee the nominal closed-loop stability (see [11]). According to the Receding Horizon Principle, only the first element \bar{u}_0 is applied to the plant. We write $\pi(\cdot, \cdot, \cdot)$ the function that inputs the current state, the current reference, and the corresponding equilibrium state and outputs the element \bar{u}_0 of the solution of (16):

$$\pi_{\text{MPC}}(x, r, x^{\text{eq}}) := \bar{u}_0. \quad (17)$$

Overall, the control policy induced by this MPC scheme reads as

$$u_k = \pi_{\text{MPC}}(x_k, r_k, x_k^{\text{eq}}), \quad (18)$$

where u_k is the input at time step k , x_k is the state of the system, r_k is the reference, and x_k^{eq} is the desired equilibrium point computed via (15) with $r = r_k$.



Fig. 9. Experiment setup

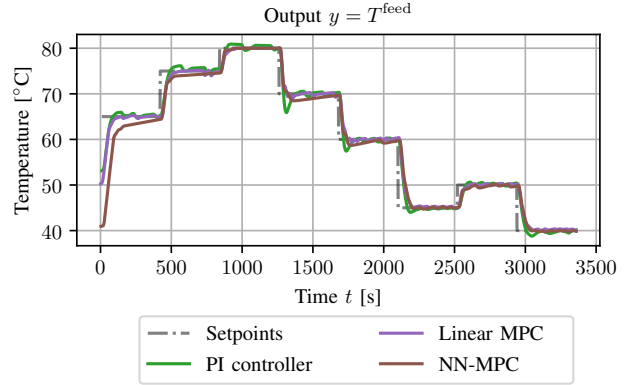


Fig. 10. Temperature profiles for the three presented controllers.

Both the Linear MPC and the NN-MPC are implemented via the presented procedure. Only the system dynamic function $f(\cdot, \cdot)$ and the output function $g(\cdot)$ in (15) and (16) differ from one controller to the other as they represent the two models discussed in Section III.

Regarding the numerical optimization of problems (15) and (16), we used the nonlinear optimization solver IPOPT [20] together with the package CasADi [21] for the symbolic expressions and automatic differentiation, and the shipped sparse linear solver MUMPS. As it is commonly done in MPC, the other components of the optimal solution of (16) are also retrieved and used as a warm start for the next iteration to make the optimization routine converge faster.

V. EXPERIMENTAL RESULTS

To compare the presented controllers, we test them on the real system (see Figure 9). The same experiment is carried out for the PI controller defined in part III-A and for the MPC scheme with both linear and NNARX models. The analog control input u is computed via (16) every $\tau_s = 6s$ while the digital control input \tilde{u} is computed every $\Delta t = 1s$ according to (1). When the solver still has not found a solution for (16) after 3s, the input is left unchanged. The results are depicted in Figures 10 and Figure 11.

To assess the performance, we use the stage cost defined in (14), which is split in two parts: the tracking cost $(y-r)^2$, and the energy cost $\lambda \cdot (u^{\text{heat}} + u^{\text{cool}})$. These costs are averaged over time from $t_0 = 10$ minutes to $t_{\text{end}} = 56$ minutes, the end of the experiment. The choice of t_0 is made to discount

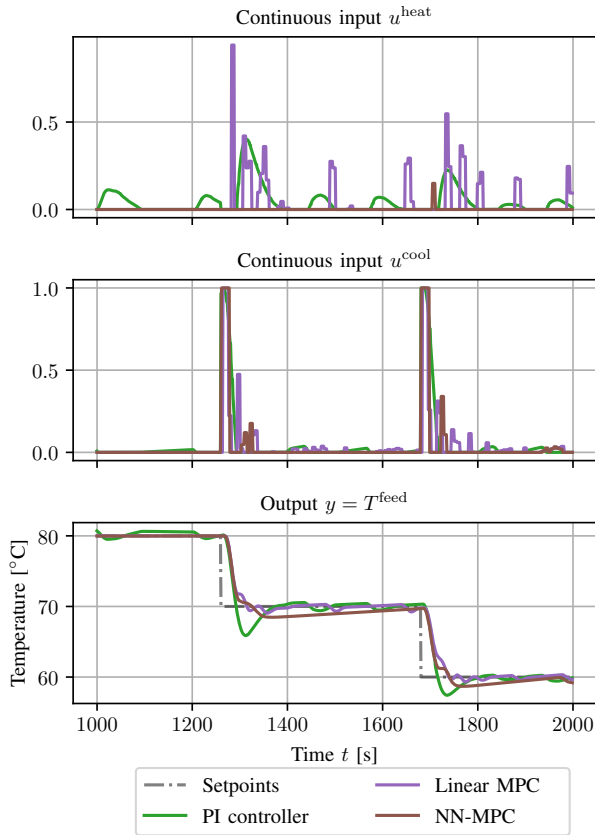


Fig. 11. Zoom-in on control performance

Controller	Tracking cost	Energy cost	Total cost
PI controller	5.30	4.48	9.78
Linear MPC	5.66	3.93	9.59
NN-MPC	5.97	2.80	8.77

TABLE I

PERFORMANCE RESULTS OF THE PRESENTED CONTROLLERS

the effects of the initial state of the system. These results are presented in Table I. The tracking performance of NN-MPC is worse compared to the other controllers. This could be attributed to increased computational effort, potentially leading to higher delays in implementing the control input. However, the PI controller overshoots (or undershoots) more than MPC controllers. It is worth noting that NN-MPC uses less control effort, which results in reduced energy costs, thereby offering economic advantages in practical TCU operations. Overall, the NN-MPC controller delivers the best performance.

VI. CONCLUSION

In this paper, we introduce a novel NNARX-based model predictive control scheme designed specifically for Temperature Control Units produced by Tool-Temp AG. Our proposed scheme outperforms compared to both the traditional PI controller and linear MPC controller, for its ability to minimize energy costs. Despite its energy efficiency, the proposed scheme maintains a relatively decent reference tracking performance.

ACKNOWLEDGEMENTS



This project has received funding from the European Union's Horizon 2020 research and innovation program under the Marie Skłodowska-Curie grant agreement No. 953348

REFERENCES

- [1] N. Cahyo, R. B. Sitanggang, H. H. Alif, and C. Hudaya, "Co-combustion characteristics of low-and medium-rank coal of the circulating fluidized bed boiler coal power plant," in *2019 IEEE 2nd International Conference on Power and Energy Applications (ICPEA)*. IEEE, 2019, pp. 282–285.
- [2] K. Rsetam, M. Al-Rawi, and Z. Cao, "Robust composite temperature control of electrical tube furnaces by using disturbance observer," *Case Studies in Thermal Engineering*, vol. 30, p. 101781, 2022.
- [3] J. Solano, E. Caamaño-Martín, L. Olivieri, and D. Almeida-Galárraga, "Hvac systems and thermal comfort in buildings climate control: An experimental case study," *Energy Reports*, vol. 7, pp. 269–277, 2021, 2021 6th International Conference on Advances on Clean Energy Research.
- [4] G. K. McMillan, *Industrial Applications of PID Control*. London: Springer London, 2012, pp. 415–461.
- [5] M. A. Johnson and M. H. Moradi, *PID control*. Springer, 2005.
- [6] Z.-S. Hou and Z. Wang, "From model-based control to data-driven control: Survey, classification and perspective," *Information Sciences*, vol. 235, pp. 3–35, 2013.
- [7] S. Hochreiter and J. Schmidhuber, "Long Short-Term Memory," *Neural Computation*, vol. 9, no. 8, pp. 1735–1780, 11 1997.
- [8] J. Chung, C. Gulcehre, K. Cho, and Y. Bengio, "Empirical evaluation of gated recurrent neural networks on sequence modeling," 2014.
- [9] H. Jaeger, "Echo state network," *Scholarpedia*, vol. 2, no. 9, p. 2330, 2007.
- [10] A. Levin and K. Narendra, "Control of nonlinear dynamical systems using neural networks: controllability and stabilization," *IEEE Transactions on Neural Networks*, vol. 4, no. 2, pp. 192–206, 1993.
- [11] J. B. Rawlings, D. Q. Mayne, and M. Diehl, *Model predictive control: theory, computation, and design*. Nob Hill Publishing Madison, WI, 2017, vol. 2.
- [12] H. R. Schindler, "Delta modulation," *IEEE Spectrum*, vol. 7, no. 10, pp. 69–78, 1970.
- [13] L. Ljung, *System Identification: Theory for the User*. Prentice Hall PTR, 1999.
- [14] R. L. Kashyap, "Maximum likelihood identification of stochastic linear systems," *IEEE Transactions on Automatic Control*, vol. 15, no. 1, pp. 25–34, 1970.
- [15] L. Simpson, A. Ghezzi, J. Asprion, and M. Diehl, "An efficient method for the joint estimation of system parameters and noise covariances for linear time-variant systems," in *2023 62nd IEEE Conference on Decision and Control (CDC)*. IEEE, 2023, pp. 4524–4529.
- [16] F. Bonassi, M. Farina, and R. Scattolini, "Stability of discrete-time feed-forward neural networks in NARX configuration," in *19th IFAC Symposium on System Identification (SYSID 2021)*, 2021.
- [17] J. Xie, F. Bonassi, M. Farina, and R. Scattolini, "Robust offset-free nonlinear model predictive control for systems learned by neural nonlinear autoregressive exogenous models," *International Journal of Robust and Nonlinear Control*, vol. 33, no. 16, pp. 9992–10009, 2023.
- [18] F. M. Bianchi, E. Maiorino, M. Kampffmeyer, A. Rizzi, and R. Jenssen, *Recurrent Neural Networks for Short-Term Load Forecasting: An Overview and Comparative Analysis*. Springer, 01 2017.
- [19] F. Bonassi, M. Farina, J. Xie, and R. Scattolini, "On recurrent neural networks for learning-based control: recent results and ideas for future developments," *Journal of Process Control*, vol. 114, pp. 92–104, 2022.
- [20] A. Wächter and L. T. Biegler, "On the implementation of an interior-point filter line-search algorithm for large-scale nonlinear programming," *Mathematical Programming*, vol. 106, no. 1, pp. 25–57, 2006.
- [21] J. A. E. Andersson, J. Gillis, G. Horn, J. B. Rawlings, and M. Diehl, "CasADi – a software framework for nonlinear optimization and optimal control," *Mathematical Programming Computation*, vol. 11, no. 1, pp. 1–36, 2019.